Journal of Experimental and Theoretical Physics, Vol. 98, No. 5, 2004, pp. 953–959.
Translated from Zhurnal Éksperimental'noĭ i Teoreticheskoĭ Fiziki, Vol. 125, No. 5, 2004, pp. 1092–1099.

PLASMA, GASES

Coulomb Broadening of the Peak of Electromagnetically Induced Transparency in Plasma

S. A. Babin, M. G. Stepanov, D. V. Churkin*, and D. A. Shapiro

Institute of Automation and Electrometry, Siberian Division, Russian Academy of Sciences, Universitetskiĭ pr. 1, Novosibirsk, 630090 Russia

**e-mail: dimkins@yandex.ru*

Received November 27, 2003

Abstract—We have measured the shape of the Autler–Townes doublet and the peak of electromagnetically induced transparency (EIT) under plasma conditions. We compare the experimental results with the calculated spectrum of the probe field of a three-level ArII Λ-scheme by taking into account Coulomb collisions. We show that the Coulomb broadening of the EIT peak is small (less than 40%), while the saturation resonance is broadened under the experimental conditions by a factor of 3. In contrast to the saturation resonance attributable to the Bennett dip in the velocity distribution of the population, the EIT peak is a coherent effect and is broadened mainly through Coulomb dephasing. *© 2004 MAIK "Nauka/Interperiodica".*

1. INTRODUCTION

A strong resonant monochromatic wave can split the energy levels and, accordingly, the emission (absorption) spectrum at transitions involving these states—an effect that has long been known and that was initially called the dynamic Stark effect [1]. Subsequently, the splitting of the spectrum into two components was called the Autler–Townes splitting (doublet). In nonlinear gas spectroscopy, field splitting is a basic effect in the classification of perturbation theory [2]; allowance for the thermal motion of particles significantly changes its spectral manifestations. For example, in a Raman scattering scheme (see inset to Fig. 1) with large Doppler broadening, the field splitting of the probe-field spectrum manifests itself only for coaxial waves in the Stokes case, i.e., at $k_\mu < k$. If only the probe level l is populated, then other nonlinear effects induced by a strong field, in particular, the saturation effect and the nonlinear interference effect (NIEF) do not show up. In this case, the absorption spectrum of the probe field describes the field splitting in pure form.

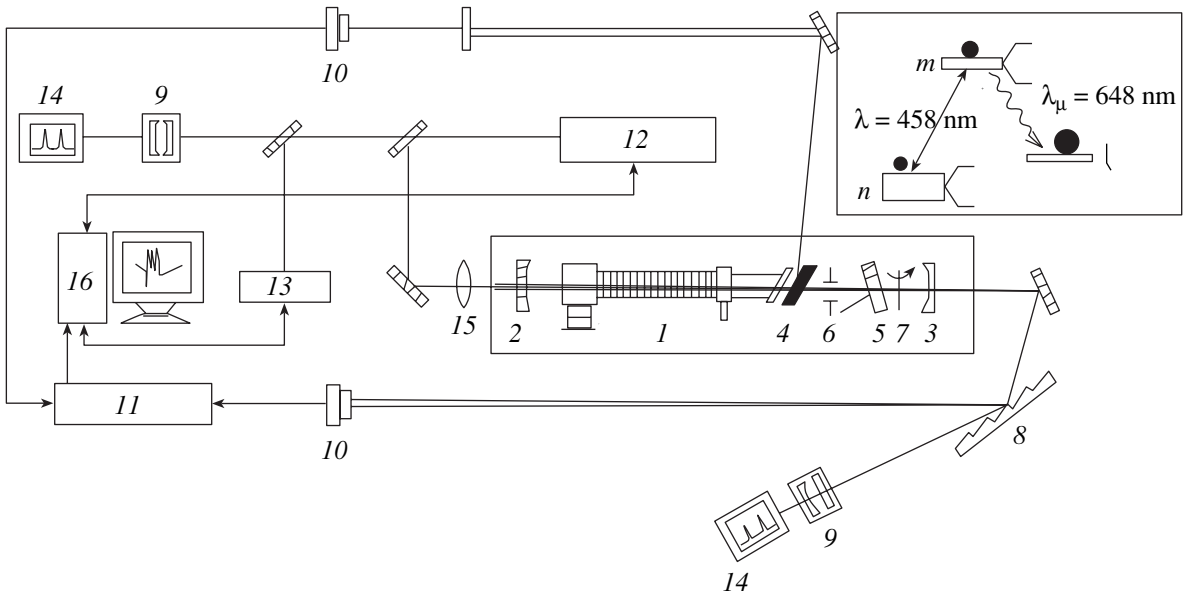

Fig. 1. Experimental setup to study field splitting: *1*—discharge tube, *2* and *3*—mirrors, *4*—Brewster plate, *5*—etalon, *6*—diaphragm, *7*—obturator, *8*—diffraction grating, *9*—scanning interferometer, *10*—photodetector, *11*—synchronous detector, *12*—tunable dye laser, *13*—wavelength meter, *14*—oscillograph, *15*—lens, and *16*—computer.

1063-7761/04/9805-0953$26.00 © 2004 MAIK "Nauka/Interperiodica"

Due to quantum interference, the field splitting of the absorption spectrum induced by a strong wave at the adjacent transition is accompanied by a significant reduction or, ideally, complete elimination of the probe-wave absorption at the frequencies corresponding to the spectral region between the split components. This effect, which was called electromagnetically induced transparency (EIT), has been actively studied in recent years (see, e.g., [3, 4] and references therein). The possibility of the elimination of light absorption under resonance conditions via the EIT effect is being actively used in various problems. In particular, the efficiency of the resonant laser frequency transformation by nonlinear optical methods [5] increases significantly, which makes it possible to use not only pulsed, but also relatively weak continuous laser emission (see, e.g., [6, 7]). In many applications, it is important to obtain the narrowest possible EIT peak, but level relaxation, and field and Doppler broadenings affect the shape of the EIT resonance [8].

In this work, we observed the Autler–Townes doublet and the EIT peak at ionic transitions in a low-temperature plasma for the first time. Ion–ion Coulomb scattering was found to also affect the shape of the peak under plasma conditions. The influence of Coulomb scattering on the shape of the resonances due to the saturation and NIEF effects under ion laser plasma conditions was studied in detail previously [9–11]. The Coulomb broadening of the EIT peak measured in this work proved to be much smaller than the Coulomb broadening of the saturation resonances. Our experimental and theoretical studies allowed us to quantitatively describe the influence of Coulomb ion–ion interaction on the field splitting and to explain the observed features.

2. EXPERIMENT

Previously, the nonlinear resonances in a Λ-scheme attributable to field splitting were experimentally studied mainly in molecular spectra (see, e.g., [12]) by using molecular Raman lasers. In this case, the observed and calculated resonance shapes are difficult to compare, because, apart from field splitting, other nonlinear effects (saturation and NIEF) contribute significantly to the total profile due to the large population of the lower level *n*. However, the measured spectrum splitting, which is proportional to the strong-field Rabi frequency

$$G = |E|d_{mn}/2\hbar$$

($|E|$ is the amplitude of the electric field, and $\hbar$ is the Planck constant), allowed the dipole moment d_{mn} of the *m*–*n* transition to be determined directly. The measurements were carried out at *G* values much larger than the relaxation constants Γ_{ij} ($i, j = m, n, l$).

As we noted above, for the profile of the Autler–Townes doublet in the Λ-scheme (see Fig. 1) to be recorded free from other nonlinear effects, the probe wave must propagate coaxially with the strong wave, and its frequency must be lower than the strong-field frequency (the Stokes case); at the same time, only the probe level *l* must be populated, while the levels *m* and *n* must be ideally empty. In contrast to thermally populated rovibrational molecular levels, ionic levels in a plasma allow the required conditions to be realized. In particular, a similar case is realized when the strong and probe fields are resonant, respectively, to the ArII laser transition and the transition to a metastable state with a large population. We chose a scheme with the following levels:

$$|n\rangle = 4s^2P_{1/2}, \quad |m\rangle = 4p^2S_{1/2}, \quad |l\rangle = 3d^2P_{3/2}.$$

The corresponding relaxation constants and Einstein coefficients (in units of 10^7 s^{-1}) are

$$\Gamma_n = 300, \ \Gamma_m = 15, \ \Gamma_l = 8, \ A_{mn} = 9, \ A_{ml} = 1.$$

The characteristic level populations in an argon laser plasma are $N_n \sim 1$, $N_m \sim 5$, and $N_l \sim 100$ (in units of 10^9 cm^{-3}) [9, 11]. Thus, the following relations hold for the level scheme chosen:

$$\Gamma_l \lesssim \Gamma_m \ll \Gamma_n \ll kv_T$$

for the relaxation constants and

$$N_l \gg N_m \gtrsim N_n$$

for the level populations.

Under argon laser plasma conditions, some of the manifestations of field splitting have been observed previously when studying the generation at coupled laser transitions in a V-scheme: when the frequency of the Stokes radiation was detuned, a decoupled resonance was observed for large detunings of the high-frequency laser field, and complex resonance structures were observed near the exact resonance for the Stokes radiation when it was tuned to the line center [13, 14]. The shape of the Autler–Townes doublet and the influence of Coulomb diffusion on it have not been investigated.

In our experiments, we studied the spectrum of a Stokes probe field in the presence of a strong field at the adjacent transition (the Λ-scheme, Fig. 1). We measured the difference between the absorption coefficients for the probe field in the absence and in the presence of a strong field that corresponded to the nonlinear correction to the probe-field work $\Delta\mathcal{P}_\mu$. For a signal of sufficient amplitude to be produced, the intensity of the strong field must be large ($G \gtrsim 100$ MHz). The intracavity field of a single-frequency 457.9-nm line ($4p^2S_{1/2}$–$4s^2P_{1/2}$) ion laser with minimum angular momentum ($j_m = j_n = 1/2$) was used to achieve these values. As a result, we measured the Autler–Townes doublet shape under argon laser plasma conditions without

the Doppler base with an accuracy high enough to make a comparison with the theory.

The experimental setup is shown in Fig. 1. An argon laser discharge tube *1* (length $l = 50$ cm, channel diameter $d = 7$ mm, and working current $I \sim 100$ A) was placed in a cavity with entrance (*2*) and exit (*3*) mirrors opaque for the generated emission, but transparent for the probe emission. Thus, there were two waves in the cavity: a standing linearly polarized generated wave and a traveling linearly polarized probe wave. Etalon *5* provided the selection of one longitudinal mode and smooth tuning of the generation frequency, while diaphragm *6* separated out the TEM_{00} mode. The cavity mirrors selected the line with a wavelength $\lambda \approx 458$ nm; the transmission losses in the cavity at this line were ≈0.3%, which provided a high field intensity inside the cavity. The emergent emission from the argon laser was directed by the mirror to a diffraction grating *8*. One order from this grating was entered into a scanning Fabry–Perot interferometer *9*, which was used to control the mode composition of the emission and to determine the strong-field detuning from the resonance, while the other order was diverted to photodetector *10*, the signal from which was the reference one for a synchronous detector *11*.

A dye laser *12* whose wavelength ($\lambda_\mu \approx 648$ nm) was recorded by a wavelength meter *13* was used as the probe-field source. The automatic frequency control (AFC) system [15] allowed us to tie the cavity mode to the selector peak and to smoothly change the probe-field frequency over a range up to 4.5 GHz. The frequency was tuned with computer *16* at discrete steps of less than 20 MHz; the step approached the emission line width (about 10 MHz). The dye-laser spectrum was recorded by the scanning interferometer *9* with a free dispersion range of 5 GHz connected to an oscillograph, which was used to control the mode composition of the emission. Before being entered into the discharge tube, the probe field was prefocused by lens *15* to provide the maximum possible field uniformity in the cavity. After the passage through the discharge tune, the probe-field beam was reflected from an additional plate *4* and diverted by the mirrors to photodetector *10* connected to the synchronous detector *11*. The angle between the beams of the probe field and the generated emission was $\sim 10^{-3}$ rad, which allowed the feedback to be avoided. The strong field was modulated at a frequency of ~1 kHz with obturator *7*; the synchronous detection at the modulation frequency allowed us to automatically subtract the Doppler base and to separate out the nonlinear corrections induced by the strong field. The personal computer *16*, to which all of the measuring instruments were connected through an ADC, was used for controlling the experiment and for synchronous data acquisition and recording.

To separate in frequency the resonances from the oppositely directed standing-wave components and to observe the field splitting induced by the traveling

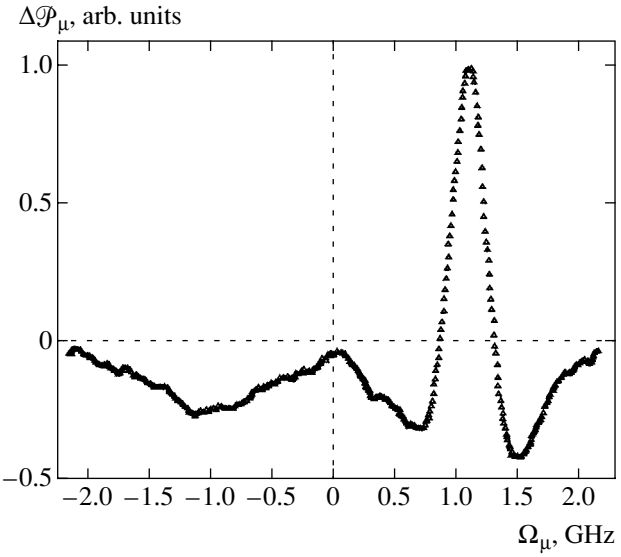

Fig. 2. Experimental profile for the nonlinear correction in the probe-field spectrum for the strong-field parameters $G \approx 100$ MHz and $\Omega \approx 1.6$ GHz.

(coaxial) wave in pure form, the strong field must be detuned from the resonance by a value larger than the population resonance width. An experimental frequency profile of the nonlinear correction to the probe-field absorption coefficient for a strong-field detuning $\Omega = \omega - \omega_{mn} \approx 1.6$ GHz is shown in Fig. 2. The negative values on the plot correspond to an increase in probe-field absorption induced by the strong field, while the positive values correspond to a decrease in absorption, which is equivalent to electromagnetically induced transparency. A sharp structure attributable to field splitting is observed for the coaxial component: the split low-amplitude absorption profile with a splitting of about 0.5 GHz and the high-amplitude EIT peak centered at a frequency $\Omega_\mu = \Omega k/k_\mu \approx 1.1$ GHz between the split components. A wide (with a FWHM of about 1.3 GHz) population resonance with a low amplitude in accordance with the level population ratio is seen symmetric about the line center at a frequency $\Omega_\mu = -\Omega k/k_\mu \approx -1.1$ GHz. The small peak at $\Omega_\mu = 0$ corresponds to the effect of higher order spatial harmonics, which is most pronounced at the exact resonance for the strong field ($\Omega = 0$) [16]; it is not considered here.

Since the contribution of the saturation effect that forms the population resonance is the same for the oppositely directed and coaxial components, we subtracted the left part of the plot ($\Omega_\mu < 0$) from its right part ($\Omega_\mu > 0$) to separate out the field splitting effect in pure form. The Autler–Townes doublet profile corrected in this way is shown in Fig. 3 together with theoretical curves computed without and with Coulomb ion–ion interaction. Since the amplitude of the doublet components for our parameters is small compared to the amplitude of the peak, it would be more precise to

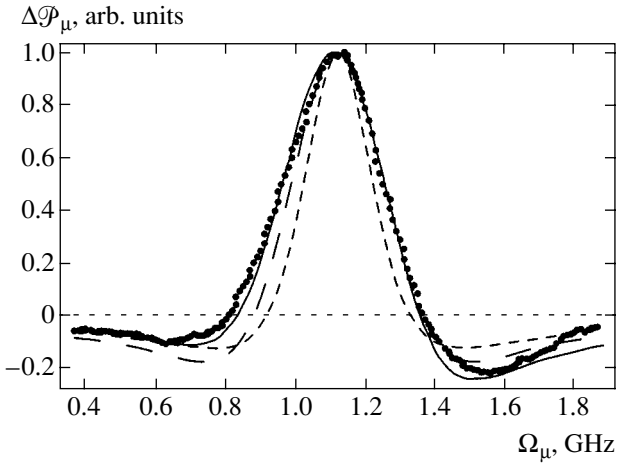

Fig. 3. Nonlinear correction in the probe-field spectrum $\Delta\mathcal{P}(\Omega_\mu)$ corresponding to the field splitting effect for the following strong-field parameters: G = 100 MHz, Ω = 1.59 GHz, and kv_T = 4.9 GHz; the short and long dashes represent the calculations using the perturbation theory without diffusion (4) and with diffusion ($\nu = 2 \times 10^7$ s^{-1}), respectively; the solid line and the dots represent the numerically calculated and experimental values, respectively.

use the term "EIT peak profile." Below, we compare the experimental and theoretical results.

3. THEORY

The nonlinear correction to the probe-field work for the Λ-scheme (Fig. 1) with $N_m = N_n \ll N_l$ calculated in the model of relaxation constants using the perturbation theory ($G \ll \Gamma_{ij}$) is [2]

$$\Delta\mathcal{P}_\mu^{(1)} = \mathcal{P}_\mu^{(1)}(0) - \mathcal{P}_\mu^{(1)}(G)$$

$$= 4\hbar\omega_\mu|G_\mu|^2|G|^2\frac{\sqrt{\pi}N_l\exp(-\Omega_\mu^2/k_\mu^2 v_T^2)(k-k_\mu)}{k^2 v_T} \quad (1)$$

$$\times \mathrm{Re}\frac{1}{(\Gamma_p - i(\Omega_\mu - k_\mu\Omega/k))^2},$$

where $|G|$ and $|G_\mu|$ are the Rabi frequencies of the strong and probe fields, k and k_μ are their wave vectors, $\Omega = \omega - \omega_{mn}$ and $\Omega_\mu = \omega_\mu - \omega_{ml}$ are the field frequency detunings relative to the corresponding resonance, $v_T = \sqrt{2T/M}$ is the thermal velocity, and N_l is the population of level l.

This formula describes the Autler–Townes doublet in absorption with the EIT peak centered at the probe-field frequency $\Omega_\mu = k_\mu\Omega/k$ with the width

$$\Gamma_p = (k_\mu\Gamma_{nl} + (k-k_\mu)\Gamma_{ml})/k. \quad (2)$$

In this approximation, the splitting $\Delta_{AT} \approx 2\Gamma_p$ does not depend on the strong-wave intensity and is determined by the relaxation constant of the forbidden transition Γ_{nl} for close magnitudes of the wave vectors. On the other hand, it is well known that in a strong field $|G| \gg \Gamma_{ij}$ (when the contribution of the relaxation constants may be ignored), the splitting for stationary atoms is determined by its Rabi frequency $|G|$, while allowance for the thermal motion leads to the addition of a scaling factor that depends on the relation between the wave vectors of the probe and strong fields (see, e.g., 12, 17]):

$$\Delta_{AT} = 4|G|\sqrt{(1-k_\mu/k)k_\mu/k}. \quad (3)$$

For an arbitrary relation between $|G|$ and Γ_{ij}, the expression for the nonlinear correction calculated in the Doppler limit ($|G|, \Gamma_{ij} \ll kv_T$) is [17]

$$\Delta\mathcal{P}_\mu = 2\hbar\omega_\mu|G_\mu|^2\frac{\sqrt{\pi}N_l\exp(-\Omega_\mu^2/k_\mu^2 v_T^2)}{k_\mu v_T} \quad (4)$$

$$\times\left(1 - \mathrm{Re}\frac{\Gamma_p - i(\Omega_\mu - k_\mu\Omega/k)}{\sqrt{(\Gamma_p - i(\Omega_\mu - k_\mu\Omega/k))^2 + \dfrac{4k_\mu(k-k_\mu)|G|^2}{k^2}}}\right).$$

In the limit $|G| \ll \Gamma_{ij}$, this expression reduces to (1), a result of perturbation theory. As the field amplitude increases, the splitting increases and is described by Eq. (3) in the limit $|G| \gg \Gamma_{ij}$.

Under the experimental conditions ($|G| \approx 100$ MHz, $\Gamma_{mn} \approx \Gamma_{nl} \approx 280$ MHz, $\Gamma_{ml} \approx 25$ MHz), the approximation of perturbation theory ($|G| \ll \Gamma_{mn}, \Gamma_{nl}$) holds well. The profile calculated using formula (4) with the field splitting (determined by the Rabi frequency $|G|$) is virtually identical to result (1) of perturbation theory—the latter curve is indicated by short dashes in Fig. 3. The FWHM of the EIT peak (and, accordingly, the splitting) in this approximation is determined by the relaxation constant of the forbidden transition

$$\Delta_{AT} \sim 2\Gamma_p \approx 2\Gamma_{nl}k_\mu/k \approx 400 \text{ MHz}.$$

The calculated curve qualitatively agrees with the experimental curve, but the width of the EIT peak in the experiment is appreciably larger (by about 40%); allowance for the field broadening yields no such broadening.

Coulomb ion scattering [9] is known to be mainly responsible for the broadening of nonlinear resonances in an ion laser plasma. This scattering is satisfactorily

described by a model of diffusion in velocity space with a velocity-independent coefficient [18, 19]:

$$D = \nu v_T^2/2, \quad \nu = \frac{16\sqrt{\pi}NZ^2e^4\Lambda}{3M^2v_T^3}, \tag{5}$$

where ν is the effective ion–ion collision frequency; $v_T = \sqrt{2T_i/M}$ is the thermal velocity; Ze and M are the charge and mass of the active ions, respectively; N is the effective number density of the perturbing ions; and Λ is the Coulomb logarithm.

The Coulomb broadening of the resonances due to saturation was studied in detail in an experiment; in particular, it was shown that the Coulomb broadening could reach a factor of 100 with respect to the radiative width for long-lived metastable levels [11]. The pattern of the diffusive broadening of population resonances is fairly easy to understand: a strong monochromatic wave produces Bennett structures with a width $\Gamma_{mn}/k \ll v_T$ against the background of a Maxwellian velocity distribution for the population of level $j = m, n$ with width v_T. Diffusion in velocity space tends to level off the nonequilibrium, causing the resonant structure to be broadened. The characteristic change in velocity increases with time t following the diffusion law

$$\Delta v_j \sim \sqrt{Dt}.$$

Over the level lifetime Γ_j^{-1}, diffusion in velocities causes the saturation resonance in the spectrum to be broadened by

$$\Delta_j = k\Delta v_j \approx \frac{kv_T}{2}\sqrt{\nu/\Gamma_j}, \quad j = m, n; \tag{6}$$

i.e., the longer the level lifetime, the larger the broadening of the saturation resonance, as distinct from the model of relaxation constants. For laser transitions, the Bennett dip is broadened predominantly at the relatively long-lived upper level. For our level scheme, the characteristic broadening of the saturation resonance is $\Delta_j/\Gamma_{mn} \sim 3$; accordingly, the width of the population resonance observed for the oppositely directed strong and probe waves centered at $\Omega_\mu \approx -1.1$ GHz (see Fig. 2) is larger by a factor of about 3 than the width of the EIT peak.

Since the EIT peak is produced by coherent effects, the Coulomb broadening mechanism in this case differs fundamentally from the broadening mechanism of population resonances. Apart from a change in the population distribution, diffusion in the velocity space also leads to dephasing (phase diffusion) of the nondiagonal density (coherence) matrix element through a random change in the ion coordinate:

$$\langle \Delta r^2 \rangle \sim \Delta v^2 t^2 \sim Dt^3,$$

which corresponds to the change in phase

$$\langle \Delta\varphi^2 \rangle = k^2 \langle \Delta r^2 \rangle \sim Dk^2 t^3.$$

The dephasing is significant when $\Delta\varphi \sim 1$. Hence, we can estimate the dephasing time scale τ_D and the related correction to the homogeneous transition width:

$$\tau_D^{-1} \sim (Dk^2)^{-1/3} \approx (\nu(kv_T)^2)^{-1/3}. \tag{7}$$

Accordingly, the correction to the width of the EIT peak (2) under experimental conditions is estimated as $k_\mu \tau_D^{-1}/k \approx 300$ MHz, which is appreciably larger than $\Gamma_p \approx 200$ MHz. This value is in conflict with the experiment, in which the observed broadening is appreciably smaller than Γ_p.

Since perturbation theory may be used to describe the experiment, the effect can be analyzed in more detail. For coaxial strong and probe waves in the Stokes case ($k_\mu < k$), we may use the nonlinear correction in the probe-field spectrum calculated using perturbation theory up to the second order in $|G|$ with diffusion in velocities [20]. Reducing the expression to a more familiar form for nonlinear spectroscopy, we obtain the line profile that corresponds to the field splitting:

$$\Delta\mathcal{P}(\Omega_\mu) = \frac{4\sqrt{\pi}\hbar\omega_\mu|G_\mu|^2|G|^2N_l(k-k_\mu)}{k^2v_T}$$

$$\times \mathrm{Re}\left\{\int_0^\infty dt \exp(i\Omega_\mu t)\Phi(t)\right\}^2, \tag{8}$$

$$\Phi(t) = \exp\{-(\Gamma_p + i\Omega k_\mu/k)t$$

$$- D(k-k_\mu)^2(k_\mu/k)^2t^3/3\}.$$

Here, we ignore the force of friction, because the resonant velocity is less than $0.4v_T$. The phase diffusion is determined not by the factor Dk^2, as suggested by estimate (7), but by a factor of $(k-k_\mu)^2k_\mu^2/k^4$ smaller quantity. Accordingly, the diffusion width of the field-splitting resonance may be expressed as

$$\Gamma_D \approx [D(k-k_\mu)^2k_\mu^2/k^2]^{-1/3}. \tag{9}$$

In the experiment,

$$k_\mu/k \approx 0.7, \quad (k-k_\mu)^2k_\mu^2/k^4 \approx 0.04.$$

Thus, the diffusion width of the field-splitting resonance, $\Gamma_D \approx 100$ MHz, is by a factor of about 3 smaller than $(Dk^2)^{1/3}$; the diffusive broadening is small, $\Gamma_D < \Gamma_p$. In the limit $D \longrightarrow 0$, the expression for the profile

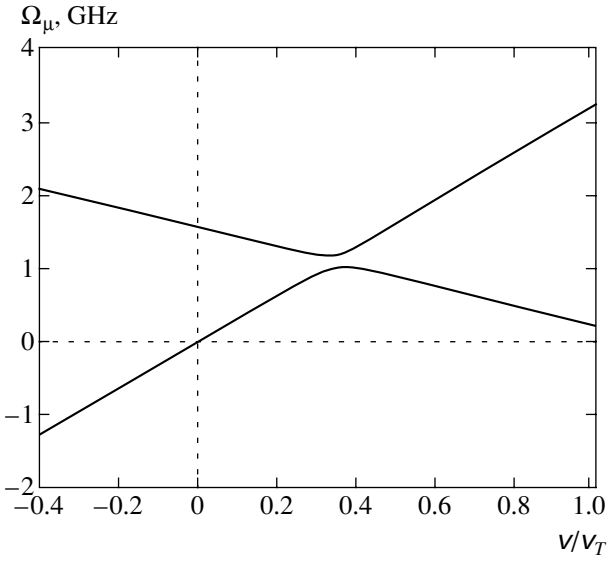

Fig. 4. Frequency branches calculated using formula (10) for the following experimental conditions: $\Omega \approx 100$ MHz and $\Omega = 1.59$ GHz.

shape reduces to (1). The result of our calculation using formula (8) of perturbation theory with Coulomb diffusion for experimental conditions is indicated by long dashes in Fig. 3. The curve satisfactorily describes the experiment; the slight deviations are attributable mainly to asymmetry in the experimental profile. The curve (solid line) calculated numerically from the system of equations for the density matrix with the diffusive and field broadenings and with the force of Coulomb friction is also shown in the figure. This curve is in even better agreement with the experiment; it also describes the asymmetry. On the right slope of the EIT peak, the results of our numerical calculations and calculations using perturbation theory with diffusion are in close agreement; deviations are clearly seen only on the left slope.

4. DISCUSSION

Our comparison of the experimental and calculated curves shows that, in contrast to the saturation resonances, population diffusion in velocities does not lead to any significant broadening of the resonance due to field splitting. A good approximation to describe the experiment is perturbation theory with diffusion; in this case, the field broadening is negligible. The opposite limiting case was analyzed in [21]: the diffusion shape of the Autler–Townes doublet components was calculated for a field splitting $|G|$ much larger than the resonance width. In this case, the diffusion width of the split components was found to be $\sim\sqrt{Dk^2/|G|}$, i.e., it decreases with increasing $|G|$, and no appreciable broadening of the resonances was observed in an experiment with strong fields in the *V*-scheme [13, 14].

Since the amplitude of the Autler–Townes doublet components in our case is small compared to the amplitude of the EIT peak, it is of considerable interest to discuss the influence of Coulomb diffusion on the shape of the EIT peak—its relative broadening under experimental conditions did not exceed 40%. Qualitatively, such a weak influence can be understood by using the pattern of frequency branches: the velocity dependence of the resonant frequencies of the split components (see, e.g., [13]). The resonant frequencies when the homogeneous width is ignored are described in our case by the expression

$$\Omega_\mu(v) = k_\mu v + (\Omega - kv)/2 \pm \sqrt{(\Omega - kv)^2/4 + |G|^2}. \quad (10)$$

The results of our calculation using formula (10) for experimental parameters are shown in Fig. 4. When averaged over velocities, the integral is accumulated in the vicinity of the extrema of the function $\Omega_\mu(v)$, called turning frequencies [13]. The size of the vicinity that gives a significant contribution is determined by the slope of the function, $d\Omega_\mu/dv$—the asymptotic behavior at large velocities is determined by the coefficients k_μ and $(k_\mu - k)$, which differ greatly in our case. Therefore, the integral is accumulated at velocities $v > 0.4v_T$ for the resonance $\Omega_\mu^1 < 1$ GHz and at $v < 0.4v_T$ for the second resonance $\Omega_\mu^2 < 1$ GHz. Given the Maxwellian distribution function, this leads to a larger amplitude of the resonance that is farther from the center of the line, as confirmed by the experiment (see Fig. 2). Formulas (1), (4), and (8) derived in the Doppler limit do not describe the asymmetry. The role of Coulomb population diffusion under these conditions reduces to the walk of particles on the frequency branch along the velocity axis in a vicinity of the order

$$\Delta v_j \sim v_T\sqrt{\nu_{ii}/2\Gamma_j}, \quad j = m, n,$$

whose size does not exceed the size of the region that contributes to the integral; therefore, this effect is weak, with the influence of diffusion on the wing shape being stronger than on the width of the EIT peak. The asymmetry in the doublet components is the result of averaging over velocities with allowance made for the finite Doppler width and is virtually independent of diffusion. Thus, the main broadening mechanism in this case is Coulomb dephasing (phase diffusion), whose effect, in turn, is weakened by a factor of $[(k - k_\mu)^2 k_\mu^2/k^4]^{-1/3} \sim 3$ under experimental conditions. As a result, the Coulomb broadening of the EIT peak does not exceed 40%.

The experiment also allows us to determine the width of the population resonance (attributable to the Bennett dip at the upper level *m*), which is observed for oppositely directed probe and strong fields—the negative detuning range in Fig. 2. It is of considerable interest to compare our result with the data of previous

experiments on the Lamb dip and the spontaneous emission spectrum (see, e.g., [9]). The FWHM of the saturation resonance in our case is $\Delta \approx 1.3$ GHz, which corresponds to a relative broadening of the Bennett dip by a factor of $\gamma = (\Delta/2\Gamma_{mn})(k/k_\mu) \approx 3.7$. This value is slightly larger than that yielded by measurements of the spontaneous emission spectrum under the same conditions (see [9]). In contrast to previous measurements, the field broadening of the population resonance in our experimental conditions was large and it could not be ignored. Our estimation of the characteristic values yields the following Coulomb, homogeneous, and field widths of the saturation resonance under experimental conditions:

$$\Delta_m = k_\mu v_T \sqrt{\nu_{ii}/2\Gamma_m} \approx 0.7 \text{ GHz}$$

($\Delta_D = 2\ln 2\Delta_m \approx 1$ GHz is the FWHM),

$$2\Gamma_{mn} k_\mu/k \approx 0.35 \text{ GHz},$$

$$\Delta_G \approx 2|G|\sqrt{2\Gamma_{mn}/\Gamma_m} \approx 0.8 \text{ GHz}.$$

Consequently, the diffusion and field widths are comparable in magnitude and are appreciably larger than the homogeneous width: $\Delta_D \gtrsim \Delta_G > 2\Gamma_{mn}k_\mu/k$. As was shown in [9, 22], the squares of the field and diffusion widths are added in these conditions; i.e., the total width may be expressed as

$$\Delta = \sqrt{\Delta_D^2 + \Delta_G^2} \approx 1.3 \text{ GHz}, \quad (11)$$

in good agreement with the measurements.

5. CONCLUSIONS

Thus, we have measured for the first time the shape of the nonlinear resonance due to field splitting under plasma conditions. Our experimental and theoretical studies of this effect at relatively low field intensities ($|G| < \Gamma_{nl}$) show that Coulomb ion–ion scattering, which leads to ion diffusion in the velocity space, affects the Autler–Townes doublet profile and the width of the EIT peak only slightly. This influence reduces to a small (about 40%) broadening of the peak and to a change in the wing shape of the split components. The main broadening mechanism is Coulomb dephasing (phase diffusion), which causes an effective increase in the homogeneous width by Γ_D described by (9). We have shown that the broadening of the saturation resonance via Coulomb population diffusion under these conditions is almost an order of magnitude larger; the field broadening in this case also gives a significant contribution.

ACKNOWLEDGMENTS

We would like to thank S.I. Kablukov, E.V. Podivilov, and S.G. Rautian for helpful discussions; O.V. Belai for help with numerical calculations; and V.V. Potapov who designed the experimental setup. This work was supported by the Russian Foundation for Basic Research (project no. 02-02-39025) and the Program of State Support for Leading Scientific Schools (project no. NSh-439.2003.2).

REFERENCES

1. S. H. Autler and C. H. Townes, Phys. Rev. **100**, 703 (1955).
2. S. G. Rautian, G. I. Smirnov, and A. M. Shalagin, *Nonlinear Resonances in Atomic and Molecular Spectra* (Nauka, Novosibirsk, 1979).
3. S. E. Harris, Phys. Today **50**, 36 (1997).
4. J. P. Marangos, J. Mod. Opt. **45**, 471 (1998).
5. S. E. Harris, J. E. Field, and A. Imamoğlu, Phys. Rev. Lett. **64**, 1107 (1990).
6. S. Babin, U. Hinze, E. Tiemann, and B. Wellegehausen, Opt. Lett. **21**, 1186 (1996).
7. A. S. Zibrov, M. D. Lukin, and M. O. Scully, Phys. Rev. Lett. **83**, 4049 (1999).
8. C. Y. Ye and A. S. Zibrov, Phys. Rev. A **65**, 023806 (2002).
9. S. A. Babin and D. A. Shapiro, Phys. Rep. **241**, 119 (1994).
10. S. A. Babin, S. I. Kablukov, M. A. Kondratenko, and D. A. Shapiro, Pis'ma Zh. Éksp. Teor. Fiz. **64**, 241 (1996) [JETP Lett. **64**, 263 (1996)].
11. A. A. Apolonsky, S. A. Babin, A. I. Chernykh, *et al.*, Phys. Rev. A **55**, 661 (1997).
12. B. Wellegehausen, IEEE J. Quantum Electron. **15**, 1108 (1979).
13. O. G. Bykova, V. V. Lebedeva, N. G. Bykova, and A. V. Petukhov, Opt. Spektrosk. **53**, 171 (1982) [Opt. Spectrosc. **53**, 101 (1982)].
14. O. G. Bykova, L. E. Grin', V. V. Lebedeva, and A. É. Sedel'nikova, Opt. Spektrosk. **64**, 1216 (1988) [Opt. Spectrosc. **64**, 725 (1988)].
15. B. V. Bondarev, S. M. Kobtsev, A. V. Karablev, and V. M. Lunin, Opt. Atmos. **2**, 1319 (1989).
16. S. A. Babin, E. V. Podivilov, V. V. Potapov, *et al.*, Zh. Éksp. Teor. Fiz. **121**, 807 (2002) [JETP **94**, 694 (2002)].
17. B. J. Feldman and M. S. Feld, Phys. Rev. A **5**, 899 (1972).
18. S. G. Rautian, Zh. Éksp. Teor. Fiz. **51**, 1176 (1966) [Sov. Phys. JETP **24**, 788 (1966)].
19. G. I. Smirnov and D. A. Shapiro, Zh. Éksp. Teor. Fiz. **76**, 2084 (1979) [Sov. Phys. JETP **49**, 1054 (1979)].
20. S. G. Rautian and D. A. Shapiro, Zh. Éksp. Teor. Fiz. **94** (10), 110 (1988) [Sov. Phys. JETP **67**, 2018 (1988)].
21. M. G. Stepanov and D. A. Shapiro, Pis'ma Zh. Éksp. Teor. Fiz. **68**, 27 (1998) [JETP Lett. **68**, 29 (1998)].
22. M. G. Stepanov and D. A. Shapiro, Zh. Éksp. Teor. Fiz. **113**, 1632 (1998) [JETP **86**, 888 (1998)].

Translated by V. Astakhov